

Phase transitions in a cellular automaton model of a highway on-ramp

This article has been downloaded from IOPscience. Please scroll down to see the full text article.

2007 J. Phys. A: Math. Theor. 40 11221

(<http://iopscience.iop.org/1751-8121/40/37/002>)

View [the table of contents for this issue](#), or go to the [journal homepage](#) for more

Download details:

IP Address: 171.66.16.144

The article was downloaded on 03/06/2010 at 06:13

Please note that [terms and conditions apply](#).

Phase transitions in a cellular automaton model of a highway on-ramp

Vladimir Belitsky¹, Nevena Marić² and Gunter M Schütz^{3,4}

¹ Instituto de Matemática e Estatística, Universidade de São Paulo, Rua do Matão, 1010, CEP 05508-090, São Paulo, Brazil

² Department of Mathematics, Syracuse University, Syracuse, NY 13244, USA

³ Institut für Festkörperforschung, Forschungszentrum Jülich, 52425 Jülich, Germany

⁴ Interdisziplinäres Zentrum für komplexe Systeme, Universität Bonn, Bonn, Germany

E-mail: belitsky@ime.usp.br, nmaric@syr.edu and g.schuetz@fz-juelich.de

Received 26 June 2007, in final form 24 July 2007

Published 29 August 2007

Online at stacks.iop.org/JPhysA/40/11221

Abstract

We introduce a lattice gas model for the merging of two single-lane automobile highways. The merging rules for traffic on the two lanes are deterministic, but the inflow on both lanes is stochastic. Analysing the stationary distribution of this stochastic cellular automaton, we find a discontinuous phase transition from a free-flow phase which depends on the initial state of the road to a jammed phase where all memory of the initial state is lost. Inside the jammed phase we identify dynamical phase transitions in the approach to stationarity. Each dynamical phase is characterized by a fixed number of relaxation cycles which is decreasing as one moves deeper into the jammed phase. In each cycle step, the number of ‘desperate’ drivers who force their way onto the main road when they reach the end of the on-ramp increases until stationarity.

PACS numbers: 05.70.Ln, 02.50.-r, 45.70.Vn, 89.75.-k

(Some figures in this article are in colour only in the electronic version)

1. Introduction

In this paper, we introduce and investigate an agent-based mathematical toy model for traffic flow in a setting where a road merges with a motorway or other major thoroughfare. Common sense (and everyday experience) tells us that a traffic jam occurs when the incoming flux of cars is too large. This phenomenon has been investigated quantitatively using detectors on German motorways. Theoretical analysis of the empirical data [1] suggests that even though congested traffic has rather intricate properties [2], the emergence of traffic jams can be explained in terms of a non-equilibrium first-order phase transition of a kind which had previously been observed in the totally asymmetric simple exclusion process (TASEP) with

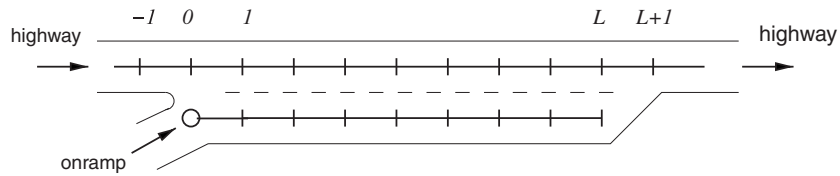


Figure 1. Cartoon picture and lattice representation of an extended on-ramp (lower road segment) merging with a highway (upper road segment). The traffic direction is from left to right. The two-lane segment is labelled by the integers $0, 1, \dots, L$. Injection onto the on-ramp is marked by the circle. The incoming highway is described by the negative integers \mathbb{Z}^- and the outgoing part by the integers $\geq L + 1$.

open boundaries [3, 4]. Later this phenomenon was argued to be generic for driven lattice gas models [5] and very recently it was proved rigorously on hydrodynamic level for certain attractive interacting particle systems [6]. This link between microscopic agent-based models defined on a lattice and a continuum description (as in Lighthill–Witham theory [7]) makes the behaviour of traffic flow interesting also from a statistical physics and a probabilistic point of view.

In the study of vehicular traffic by interacting particle systems [8, 9], the road is discretized into segments and the particles hopping on such a lattice in discrete or continuous time represent the motion of cars. Very often exclusion rules are considered where each lattice site can accommodate at most one particle, i.e. a single site represents a road segment of the length of a typical car. In [10, 11] coupled TASEPs with open boundaries are used to describe a junction where one road meets another road at some lattice site, giving rise to a variety of stationary traffic phases that can be deduced from the behaviour of the standard single-lane TASEP. In [12–14] particles are injected at single lattice sites of a long lattice to describe the effect of an on-ramp of the length of a single car. Other work [15–20] considers extended on-ramps as we do here. However, all previous work focuses on metastability or stationary behaviour. Relaxation phenomena which may occur as a result of a rapid change of traffic conditions have not yet been studied within the lattice gas approach.

Since we are interested in generic features of the large-scale behaviour that emerges from ‘microscopic’ interaction rules between particles, we keep our mathematical model as simple as possible. In line with the agent-based cellular automaton (CA) approach to traffic flow, we define a cellular automaton where the dynamics on the infinitely extended single-lane main road are those of Wolfram’s deterministic CA184 [21]. The on-ramp is represented by one lane of a two-lane road segment of L sites, see figure 1 for illustration. The lane-changing rules are asymmetric and inspired by, but different from those of the deterministic two-lane CA named TL184 [22].

It is clear that a fully deterministic description of the motion of cars cannot capture the effect of inevitable fluctuations in the inflow of cars on a real highway. Thus, our CA is made stochastic by introducing random initial conditions and one stochastic boundary at the entrance of the on-ramp (random inflow from the secondary road). This stochastic CA (SCA) is described in detail in the following section. Our goal is to investigate how the inflow from the secondary road through the on-ramp causes traffic jams, assuming that initially the main road is in a free-flow state. We study the phase diagram, i.e. the dependence of the stationary current and traffic density on the input rate of particles and initial occupation on the main road in the thermodynamic limit $L \rightarrow \infty$. Moreover, we investigate for large, but finite system size how stationarity is approached if initially the on-ramp is empty. We obtain the following

two main results. (i) There is a phase transition from a free-flow phase to a jammed phase for sufficiently large inflow. (ii) There are dynamical phase transitions inside the jammed phase. Each dynamical phase is characterized by a fixed number of relaxation cycles through which the system approaches stationarity.

For the derivation of our results we use heuristic hydrodynamic arguments, based on the law of large numbers in the thermodynamic limit of large L . In order to demonstrate what bearing asymptotic results may have for finite systems, we also present Monte Carlo simulation data obtained from single realizations of the process on lattices of size $L = 100$.

Since some properties of our model are inherited from CA184, we first review in the following section its definition and some rigorously established results. Then we present our model and the initial states we are interested in. In section 3, we derive the phase diagram. In section 4, we discuss the relaxation process and present Monte Carlo simulation results. We conclude in section 5 with some comments on our results and various related open problems that deserve further research.

2. The SCA on-ramp model

2.1. A very brief review of CA184

In order to facilitate the definition and discussion of our model, we collect here some results on CA184 which is defined as follows. Each site on \mathbb{Z} is occupied by at most one particle (exclusion principle). The particle evolution is in discrete time $\{1, 2, \dots\}$ such that each particle that has a vacant site to its right is first marked. Then (in the same time step) each marked particle jumps one lattice unit to the right [21], and the mark is removed. This operational definition, useful for computer implementation of the dynamics, is equivalent to saying that in each time step each particle that has a vacant site as its right neighbour jumps one lattice unit to right.

Let a particle distribution on \mathbb{Z} be translation invariant (i.e. the distribution does not change, if it is shifted along \mathbb{Z}) and let it either have no neighbouring particles or have no neighbouring vacancies. Then, in both cases, this distribution is also time invariant for CA184. We shall refer to time-invariant distributions as *stationary* distributions; for details see e.g. [23, 24]. At particle densities up to $1/2$, the system is said to be in the *free-flow phase* since each particle moves at each time step due to the absence of particle pairs. At densities larger than $1/2$ the system is said to be in the congested phase, since in any large enough region there are always some particles that cannot move in a given time step.

Let us denote by $j(\rho)$ the particle current in a stationary distribution with particle density ρ . It may be easily derived (for a formal proof see [22], although this result had been known much before) that

$$j(\rho) = \begin{cases} \rho & \text{if } \rho \leq 1/2 \\ 1 - \rho & \text{if } \rho \geq 1/2. \end{cases} \quad (1)$$

This current–density relation, called fundamental diagram in traffic engineering, also plays a crucial role for the discussion of our on-ramp SCA.

It is interesting to consider a non-translation invariant distribution where the left part of the system is in the free-flow phase with density $\rho_- \leq 1/2$ and the right part is in the congested phase with density $\rho_+ > 1/2$. It has been established in recent work that the transition point from the free-flow region to the congested region can be defined and tracked on microscopic lattice scale at all times [25]. At each time step, there is always a unique particle that may be regarded as marking the end of a traffic jam which on a macroscopic scale corresponds to a shock discontinuity. It connects the two domains with constant densities ρ_1 and ρ_2 and

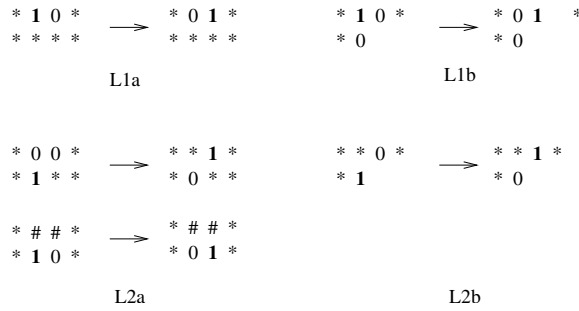


Figure 2. All allowed moves of a car (symbol 1) onto an empty site 0 as given by the rules R1 in lane 1 (top two figures L1-a, L1-b) and lane 2 (bottom two figures L2-a, L2-b). The asterisks indicate unspecified occupation, on which the jump event does not depend. The pair of hashes signifies that at least one of the two sites is occupied.

performs a random motion with average speed

$$v_s = \frac{j(\rho_-) - j(\rho_+)}{\rho_- - \rho_+}. \quad (2)$$

This speed becomes deterministic in the hydrodynamic limit where the lattice spacing becomes 0 and the density and current become deterministic quantities. On a macroscopic scale this result follows from particle conservation and is generally valid, provided a shock exists and remains stable under the time evolution of the particle system. The existence of a *microscopic* shock in CA184 motivates our use of it as a building block for an on-ramp traffic model.

On the other hand for $\rho_- > 1/2$ and $\rho_+ < 1/2$, an initial shock is not stable. Instead, an intermediate domain with density $1/2$ develops, with one discontinuity moving deterministically (speed -1) to the left, and another discontinuity moving deterministically (speed $+1$) to the right. Hence, the outflow from a congested regime into a free-flow regime is maximal and the congested regime shrinks in size. A high-density downward shock with $\rho_- > \rho_+ \geq 1/2$, however, does remain stable and travels with speed -1 backwards. Likewise, a low-density downward shock with $1/2 \geq \rho_- > \rho_+$ is stable and travels with speed $+1$ forward.

2.2. The main road and the on-ramp

With CA184 in mind we can define the SCA model for an on-ramp, see figure 1. The single-lane main road is modelled by the set of integers \mathbb{Z} . The on-ramp is represented by the set of integers in the finite interval $[0, L]$. The integers of the main road, or simply highway or *lane 1*, are denoted by $\dots, -1_1, 0_1, 1_1, \dots$. The integers of the on-ramp or *lane 2*, will be denoted by $0_2, 1_2, \dots, L_2$. Cars are modelled by particles satisfying the exclusion principle (at most one particle per site). Their motion is defined by dynamical rules for the particle evolution on the sites of lanes 1 and 2, as given below. We shall refer to the set $(L+1)_1, (L+2)_1, \dots$ as the outgoing lane (or highway) and to the negative integers \mathbb{Z}_1^- as the incoming lane (or highway).

2.3. Cars and their motion

The rules for particle motion in our present model are illustrated in figure 2 where all possibilities in which a car can move are shown. In the following precise description, the rules (L1-a,b) mimic cars on the main road. Each car advances if there is no other car in front of

it (rule (L1-a) as in CA 184). Cars do not slow down to let space for a car from the on-ramp to enter the main road, except at the end of the on-ramp (rule (L1-b)). The rules (L2-a,b) mimic the behaviour of cars that have entered the on-ramp. Each of these cars prefers to enter the main road as soon as possible, rather than to advance along the on-ramp. However, this happens only if it does not prevent the free motion of cars on the main road. Otherwise, the car will keep moving along the on-ramp obeying the CA 184 exclusion principle (rule (L2-a)). When a car has reached the end of the on-ramp, it becomes ‘desperate’ and changes to the main road even though this change may force a car on the main road to brake (rule (L2-b)).

More precisely, these rules may be stated as follows.

(R1) (Particle jumps) Particles change their positions at times $1, 2, \dots$ according to the following rules.

(L1-a) If there is a particle at time $t - 1$ at a site $i_1 \neq L_1$, then it checks whether the site $(i + 1)_1$ is empty at time $t - 1$, and if yes, it will jump to $(i + 1)_1$ at time t ; otherwise, it will stay at i_1 at time t .

(L1-b) If there is a particle at time $t - 1$ at the site L_1 , then at time t it will jump to $(L + 1)_1$ provided at time $t - 1$ both sites $(L + 1)_1$ and L_2 are free of particles, otherwise, it will stay at L_1 .

(L2-a) If there is a particle at a site $i_2 \neq L_2$ of lane 2 at time $t - 1$, it checks whether the sites i_1 and $(i + 1)_1$ are empty at time $t - 1$; if yes, it will jump to $(i + 1)_1$ at time t . Otherwise, the particle checks whether the site $(i + 1)_2$ is empty at time $t - 1$; if yes, it will jump to $(i + 1)_2$ at time t , otherwise, it will stay at i_2 at time t .

(L2-b) A particle that is at the site L_2 at time $t - 1$, checks whether the site $(L + 1)_1$ is empty at time $t - 1$. If yes, it jumps to $(L + 1)_1$ at time t , otherwise it keeps its position at time t .

(R2) (Particle input) A new particle may appear on the on-ramp at 0_2 at each time $1, 2, \dots$ according to the following stochastic rule: if there is no particle at time $t - 1$ at site 0_2 , then a new particle will appear at this site at time t with probability p_2 .

The real number $p_2 \in [0; 1]$ is one of the model’s parameters.

2.4. The initial particle configuration

In order to complete the description of the model, we specify the initial distribution of particles. We recall that our goal is to investigate how inflow onto the on-ramp causes traffic jams. This suggests that the model should be considered starting from the moment when the first particle enters the on-ramp. Accordingly, we assume that lane 2 is totally free of particles at time 0. Moreover we assume that there are no traffic jams initially on the main road; hence particles are put at time 0 on lane 1 with density $\rho \leq 1/2$ according to the following rule: the particle distribution is translation invariant and the number of vacant sites between particles are independent random variables $1 + X$, where X is a geometric random variable with parameter p_1 (i.e. $\mathbb{P}[X = k] = p_1(1 - p_1)^k, k = 0, 1, 2, \dots$). The real number $p_1 \in (0; 1)$ is the second parameter of the model. The invariance with respect to translations and the minimal gap size 1 between consecutive cars ensure that this distribution models a stable free car flow on the main road in the absence of the on-ramp. In terms of p_1 , we have

$$\rho = \frac{p_1}{1 + p_1}. \quad (3)$$

The geometric gap size distribution is chosen for convenience in both numerical and rigorous treatments of the problem. We believe that the phase transition discussed below would occur for any X with finite mean.

3. Phase diagram

3.1. Microscopic consequences of the merging rules

The lane-changing rules along the on-ramp have several microscopic consequences that are important for deriving the coarse-grained macroscopic behaviour.

- (P1) *Particle distribution on lane 1 after the on-ramp.* If at any time t a particle jumps to $(L+1)_1$ (independently, on whether it has come from lane 1 or lane 2), then it will be in a free-flow phase at all times $\geq t+1$. Thus, the most ‘dense’ configuration on the outgoing lane $\{(L+1)_1, (L+2)_1, \dots\}$ is the particle–hole interchanging configuration with density $\rho = 1/2$ and current $j = 1/2$. If lane 1 has no vacancy pairs on all sites up to L_1 , then this maximal-density state is realized on the outgoing lane.
- (P2) *Particle distribution on lane 2.* All the particles at all times are almost in the free-flow phase. Here the proviso ‘almost’ means that at each time t , there may be at most one particle that cannot jump at time t . It may be at L_2 (the end of lane 2) because its jump may be blocked due to the presence of a particle at $(L+1)_1$. However, this particle cannot be blocked for more than one time step because of rule (L2-b). Alternatively, a blocked particle may be at any other site of lane 2. If such a particle exists, it forms a particle block of size 2, and therefore also cannot be blocked for more than one time step. Since moreover a particle at a site $i_2 < L_2$ can be blocked only as the result of an alternating particle–hole string trailing a blocked particle at L_2 some time steps earlier, the region of lane 2 to the right of this block at i_2 is occupied by the particle–hole interchanging configuration such that if L_2 is occupied, then L_1+1 is empty and *vice versa*. (For this reason, no second blocked particle can be generated at L_2 before the other blockage has disappeared.) If a block of size two has two vacant sites as left neighbours, the block disappears in the next time step and no blocked particles exist until a new blocked particle may be generated at L_2 .
- (P3) *Lane change for high density on lane 1.* If there are no vacancy pairs on lane 1 up to site L_1 , then particles injected on lane 2 cannot move to lane 1 before reaching the end of the on-ramp. The injection rule (R2) then generates gap sizes $1+X$ between consecutive particles, where X is geometrically distributed with parameter p_2 . The length of such a random sequence is limited by a single block of size 2 as discussed in (P2).

Property (P2) implies that if the merging of the two lanes at the end of the on-ramp causes a traffic jam, then this traffic jam will develop and propagate backwards on the main road—not on the on-ramp. This is an interesting consequence of the behaviour of desperate drivers in our model and the asymmetric lane-changing rule which forbids returning from the main road onto the on-ramp. This property also allows us to truncate the on-ramp at the entrance to the main road and describe the influx by a stochastic boundary, rather than modelling the full secondary road by another infinite integer lattice with some random initial configuration of particles.

The same free-flow property implies that in the limit of large L , there is a stationary inflow

$$\alpha = \frac{p_2}{1+p_2} \quad (4)$$

of particles onto the two-lane segment of the highway.

3.2. Stationary state

With these preparations, we are in a position to deduce the phase diagram of the on-ramp model. To fix notation, we denote by $\rho_{\text{in}}, \rho_{1,2}, \rho_{\text{out}}$ the stationary densities in the various

segments of the road. j with the corresponding subscript denotes the stationary current in the respective segment as given by (1).

First we make some trivial observations. (i) Since initially lane 2 is empty, the particles initially in the positive segment of lane 1 do not interact with any particle injected at positive time. They disappear into the outgoing highway after at most L steps. Hence, we may delete all particles which are on \mathbb{Z}^+ at $t = 0$ without changing the long-time behaviour of the two-lane segment. (ii) Because of the geometric initial distribution on lane 1 we may regard site 0_1 as a source of particles entering the two-lane segment in the same fashion as site 0_2 is a source of particles for lane 2, as long as no back-moving traffic jam blocks the hopping of a particle from -1_1 onto 0_1 . (iii) Any blocking of the forward motion of any particle may occur not earlier than after L steps, when the first injected particle may have reached the end of the on-ramp. Hence initially (at least up to time L) there is a free inflow of particles into the two-lane segment with total current $j_0 = \rho + \alpha$.

Now note that the two-lane segment with stationary currents $j_{1,2}$ on each lane cannot support a stationary current $j := j_1 + j_2$ larger than $1/2$ since stationarity requires

$$j_1 + j_2 = j_{\text{out}}. \quad (5)$$

The current j_{out} of the outgoing lane 1 is limited by $1/2$ since this is the maximal current that CA184 can support. Hence for $\rho + \alpha > 1/2$, a traffic jam must develop on lane 1 that moves backwards and eventually reaches site 0_1 . Then it may block further input and eventually generate a stationary situation. It is therefore clear that for $\rho + \alpha > 1/2$, the initial free-flow situation is unstable and the stationary system is in a congested phase. Hence, the first task at hand is to determine whether the initial free-flow scenario $\rho + \alpha \leq 1/2$ is stable and to determine the stationary densities $\rho_{1,2}$ as a function of the system parameters. It is convenient to describe the phase diagram in terms of α and ρ rather than p_1 and p_2 . We shall rely heavily on hydrodynamic arguments in terms of mass transport by stationary currents. Corrections vanishing in system size L are ignored in the following discussion.

First we investigate the behaviour at the beginning of the on-ramp, assuming $L = \infty$. A particle that has entered the on-ramp on site 0_2 will move onto lane 1 according to rule L2-a, i.e. provided both sites 0_1 and 1_1 are empty. The distribution of particles on lane 1 is geometric as described above and uncorrelated with the injection of particles. Elementary computation then gives the probability $Y_1(00)$ to find two neighbouring vacant sites on lane 1 (and hence the jump probability of a particle that has just been injected) as

$$Y_1(00) = \frac{p_1}{1 + p_1} \sum_{n=1}^{\infty} n p_1 (1 - p_1)^n = \frac{1 - p_1}{1 + p_1}. \quad (6)$$

In terms of the particle density, this can be written as $Y_1(00) = 1 - 2\rho$ for $\rho \leq 1/2$.

For an infinite on-ramp the law of large numbers then guarantees that with the given initial distribution on the incoming highway, a fraction 2ρ of all injected particles will remain on lane 2. Anticipating the discussion of the dynamics given in the following section we extend this argument to the stationary distribution and replace the initial value ρ by the (as yet unknown) stationary density ρ_{in} , provided that $\rho_{\text{in}} \leq 1/2$. For $\rho_{\text{in}} > 1/2$, no injected particles can move from lane 2 onto lane 1 before reaching the end of the on-ramp. Since the probability to have a particle on site 0_2 is α by definition, we conclude that

$$\rho_2 = \begin{cases} 2\alpha\rho_{\text{in}} & \text{for } \rho_{\text{in}} \leq 1/2 \\ \alpha & \text{for } \rho_{\text{in}} > 1/2 \end{cases} \quad (7)$$

is the stationary density on lane 2. The corresponding stationary current on lane 2 is then

given by

$$j_2 = \rho_2. \quad (8)$$

Since lane 2 is always in the free-flow phase (property (P2)), we expect that these expressions also remain valid up to finite-size corrections (due to fluctuations) for an ensemble of large, but finite systems.

The next step is to determine the stationary density on lane 1. For sufficiently low ρ and α , the particles that initially move from lane 2 to lane 1 after injection keep lane 1 in the free-flow phase. Its current is given by the sum of the incoming current $\rho_{\text{in}} = \rho$ and the added current $(1 - 2\rho)\alpha$, contributed by the particles coming from lane 2. We argue that this sum is the stationary current j_1 on lane 1 (and correspondingly $j_2 = 2\alpha\rho$ is the stationary current on lane 2) as long as $\alpha + \rho = j_1 + j_2 = j_{\text{out}} \leq 1/2$. This free-flow scenario is stable because even though a blocked particle that may be generated at the end of the on-ramp leads to a back-moving traffic jam, this traffic jam dissolves quickly. It has only a finite average length (not scaling with the system size), since a growth of a congested domain with density $\rho_{\text{jam}} \geq 1/2$ over a macroscopic region cannot be sustained by the incoming flux of particles, except as a result of a rare fluctuation. To create a macroscopic jam of length xL (where $0 < x \leq 1$), a number of $(\rho_{\text{jam}} - \rho_1)xL$ excess particles have to be carried into the system during $O(L)$ time steps. However, such a fluctuation in the influx is exponentially improbable in L ; see property (P3) combined with the fact of the geometric initial distribution on lane 1. Hence, the entire system (with the possible exception of a fluctuating congested segment of a finite average size) is in the free-flow phase if $\alpha + \rho \leq 1/2$.

Assume now $\alpha + \rho > 1/2$. Recall that according to (P2) lane 1 must be congested, i.e. have density $\rho_1 > 1/2$. By (P1) this implies an outgoing stationary current $j_{\text{out}} = 1/2$, and stationarity then gives $j_1 = 1/2 - j_2$ with density $\rho_1 = 1 - j_1 = 1/2 + \rho_2$. Moreover, a traffic jam on lane 1 with a congested region of density $> 1/2$ moves backwards into the incoming lane, see (2). Hence $\rho_{\text{in}} = \rho_1$.

With (7) this gives the full dependence of the stationary densities of the two-lane segment as a function on the system parameters as follows.

(i) *Free-flow phase* $\alpha + \rho \leq 1/2$:

$$\rho_{\text{in}} = \rho \quad (9)$$

$$\rho_1 = \alpha + \rho - 2\alpha\rho \quad (10)$$

$$\rho_2 = 2\alpha\rho \quad (11)$$

$$\rho_{\text{out}} = \alpha + \rho. \quad (12)$$

The total stationary current is the sum of the two input currents, $j = \alpha + \rho$. The stationary currents in the individual road segments follow from (1).

(ii) *Congested phase* $\alpha + \rho > 1/2$:

$$\rho_{\text{in}} = 1/2 + \alpha \quad (13)$$

$$\rho_1 = 1/2 + \alpha \quad (14)$$

$$\rho_2 = \alpha \quad (15)$$

$$\rho_{\text{out}} = 1/2. \quad (16)$$

The total stationary current is maximal, $j = 1/2$; the stationary distribution does not depend on the initial density ρ .

4. Dynamical phase transitions in the congested phase

4.1. Microscopic and hydrodynamic description of boundary-induced phase transition in single-lane CAs

As an introductory note to the dynamical analysis of the stationary phase diagram of the on-ramp model, we recall some properties of single-lane SCAs with L sites and open boundaries where particles are injected (left boundary) and extracted (right boundary), according to some stochastic rules. We assume these boundary dynamics to be chosen such that particle injection creates a growing free-flow segment of density ρ_- in an initially empty semi-infinite chain extending from site 1 to $+\infty$. The extraction mechanism is chosen to generate a growing congested segment of density ρ_+ in an initially full semi-infinite chain extending from $-\infty$ up to site L . Such SCAs have first been studied in [26] and subsequently by other authors [27–30]. Two-component generalizations were considered in recent work [31, 32]. Interestingly, the current–density relation (1) arises also in the CA with sublattice parallel update studied rigorously in considerable detail in [26]. Further analysis reveals the following properties which we also expect to be valid for CA184 with suitably chosen open boundaries, and indeed (except for the details of the current–density relation) also for stochastic time-evolution schemes for totally asymmetric simple exclusion processes [33].

Consider an initial shock distribution with densities ρ_{\pm} such that its distribution is stationary except close to the shock position. For sufficiently large L , a suitably defined shock marker [25] then performs a biased random motion until it hits one of the boundaries. The average speed v_s of the shock follows from (2). Its sign has its origin in the balance of the currents $j_- = \rho_-$ of particles entering at the left boundary and $j_+ = 1 - \rho_+$ of particles leaving the system at the right boundary.

For $j_- > j_+$ (corresponding to $\rho_- > 1 - \rho_+$) the incoming flux brings (on average) more particles into the system than the outgoing flux can remove. Hence, the number of particles in the system grows and the shock moves to the left. When the shock reaches the boundary, it reduces the incoming microscopic flux for some finite time because once in a while injection attempts are rejected due to the enhanced probability of finding site 1 occupied. This reduced influx causes the shock to drift away from the boundary to the right. However, as soon as this happens, particles flow in again unhindered, driving the shock again back towards the left boundary. In order to allow for the shock to move a large distance k forward into the bulk, it is necessary that there is an excess of vacancies (either enhancing the flux in the high-density branch of the shock or reducing the flux in the low-density branch) such that v_s can be positive for a sufficiently long time. The probability of generating such an excess of vacancies (compared to the average) is exponentially small in k . Therefore, the probability of finding the shock marker in the bulk decays exponentially in its distance from the boundary. Consequently for large L , the expected number of particles in the system is $\rho_2 L$. The system is in a high-density regime, determined by the outflow at the right boundary.

Conversely, if $j_- < j_+$, the incoming flux cannot compensate the loss of outgoing particles at the right boundary and the shock moves left. Similar arguments lead to the conclusion that for large L , the expected number of particles in the system is $\rho_- L$. Hence, the system is in a low-density regime governed by the influx at the left boundary. This may be summarized in the following expression for the bulk density ρ in the thermodynamic limit $L \rightarrow \infty$:

$$\rho = \begin{cases} \rho_- & \text{for } \rho_- < 1 - \rho_+ \\ \rho_+ & \text{for } \rho_- > 1 - \rho_+. \end{cases} \quad (17)$$

Since there is a discontinuous change of the stationary bulk density, we say that there is

first-order non-equilibrium phase transition. Formula (17) defines the phase diagram in the two-dimensional parameter manifold.

This heuristic dynamic discussion of the phase transition implies properties of the stationary distribution which are proved rigorously both for the original sublattice CA in [26] and later also for CA184 with open boundaries [27, 28]. We wish to stress that our reasoning relies on the existence of a microscopic shock (which is proved for CA184 in [25]), but is otherwise essentially hydrodynamic in nature.

On the coarse-grained hydrodynamic level, the phase transition detailed above may be rephrased as follows. One defines a coarse-grained density as a space average over a suitable chosen region around the lattice site k that becomes infinite in the limit $a \rightarrow 0$ of vanishing lattice spacing a , but is only a point $x = ka$ on a macroscopic scale. In this limit, the particle distribution on the lattice is described by density profile $\rho(x, t)$ in continuous space. The lattice of L sites becomes an interval $[0, L'] \in \mathbb{R}$ of a finite macroscopic length $L' = aL$. The particle densities introduced earlier somewhat loosely as space averaged (but still fluctuating quantities) become deterministic because of the law of large numbers. To describe the dynamics, one also rescales time and introduces a finite macroscopic time $t' = ta$. As a consequence of taking the microscopic time to infinity, we may infer local stationarity at x as long as we are a macroscopic distance away from any shock discontinuity. Hence in a (macroscopic) point of density ρ , the corresponding current is $j(\rho)$. To recover the phase diagram discussed above, one considers an initial density profile with a shock located some point x_0 and applies arguments entirely analogous to those above. They yield the motion of the shock and hence the phase diagram.

One can also consider an initially empty lattice, corresponding to $\rho(x, 0) = 0$. Then one expects for CA184 up to $t' = L'$ an evolving step-function profile $\rho(x, t) = \rho_-$ for $0 < x < t'$ and $\rho(x, t) = 0$ for $t < x < L'$. The right boundary can support the current $j(\rho_-) = \rho_-$ in the approaching low-density domain provided that $j(\rho_+) > \rho_-$. If this is the case the density remains stationary after $t' = L'$, in agreement with the prediction (17). Otherwise, a back-moving shock of the form assumed above (with a high-density domain ρ^+) evolves and we are back at the previous discussion which leads to (17).

4.2. Relaxation of the on-ramp model in the free-flow phase

Hydrodynamic theory provides the key notions required for analysing the asymptotic properties of the on-ramp model. In order to describe the relaxation process from the initial condition, we now use the hydrodynamic description introduced above. In order not to burden notation with primes whenever reference to the length of the on-ramp or time is made, we drop the primes and from now on take L and t to be rescaled macroscopic quantities, unless otherwise stated. In the initial state, the density on lane 1 is given by $\rho_1(x, 0) = \rho$. On lane 2, we have $\rho_2(x, 0) = 0$ for $0 \leq x \leq L$. Outside this range, $\rho_2(x, t)$ is not defined.

Under hydrodynamic scaling, the initial lane-changing process takes place at $x = 0$ and leads to the following initial stage of the time evolution. For a pictorial presentation, see figure 3.

- (1) *Loading stage* $0 < t < L$. During this time interval, the flux into the two-lane segment from the incoming highway is $j_0 = \rho$ and the flux from the on-ramp is α . Hence, a forward-moving step-function wave penetrates lane 2 due to injection at $x = 0$. According to (6), lane change induces a similar wave on lane 1 such that

$$\rho_1(x, t) = \begin{cases} \rho & x < 0 \\ \alpha + \rho - 2\alpha\rho & 0 < x < t \\ \rho & t < x \end{cases} \quad (18)$$

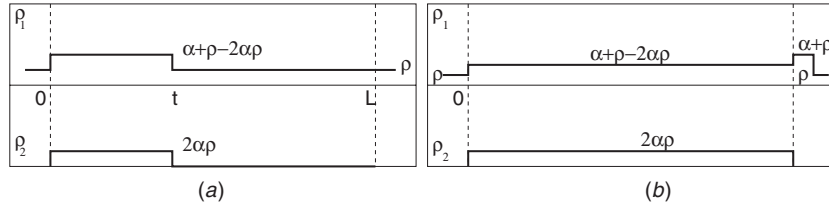


Figure 3. Schematic picture of the relaxation process under hydrodynamic scaling in the free-flow regime. In the initial loading process up to time $t = L$, lane 2 is filled and a density wave is induced on lane 1 due to lane changing at the beginning of the on-ramp (a). For $t > L$ the two-segment is stationary and the density wave proceeds indefinitely on the outgoing lane 1 (b).

and

$$\rho_2(x, t) = \begin{cases} 2\alpha\rho & 0 < x < t \\ \rho & t < x < L. \end{cases} \quad (19)$$

Note that the total flux $\alpha + \rho$ inside the forward-moving density wave, i.e. inside the domain $0 < x < t$, matches the total incoming flux as required by local stationarity away from the density discontinuity.

- (2) *Stationary regime $t > L$.* When the forward-moving wave hits the end of the on-ramp, nothing special occurs on a hydrodynamic scale. Microscopic-congested regions that may appear for a finite time vanish under hydrodynamic scaling. The complete two-lane segment becomes stationary. The evolution is given by

$$\rho_1(x, t) = \begin{cases} \rho = \rho_{\text{in}} & x < 0 \\ \alpha + \rho - 2\alpha\rho = \rho_1 & 0 < x < L \\ \alpha + \rho = \rho_{\text{out}} & L < x < t \\ \rho & t < x \end{cases} \quad (20)$$

and

$$\rho_2(x, t) = 2\alpha\rho = \rho_2. \quad (21)$$

In the limit $t \rightarrow \infty$, the entire highway is stationary.

4.3. Relaxation cycles in the congested phase

The relaxation process in the congested phase is far more subtle. The novelty is the back-moving traffic jam that develops on lane 1 around microscopic time $t \approx L$. To get some insight, we return briefly to a microscopic description of the dynamics in two special limiting cases where either the initial distribution (case a) or the injection (case b) is deterministic.

- (a) Suppose that $\rho = 1/2$, i.e. lane 1 is initially half-filled (alternating particle-vacancy sequence). According to property (P3) any particle injected on lane 2 will eventually move onto site $(L + 1)_1$ of the main road, causing the particle on L_1 to break. Hence, the stationary density on lane 2 is $\rho_2 = \alpha \leq 1/2$ and the current is $j_2 = \alpha$.

The stationary density on lane 1 may be derived by employing the following tools.

- (1) We tag all particles injected on lane 2 and call them red particles (as opposed to ‘black’ untagged particles initially on lane 1). (2) When a black particle becomes the left neighbour of a red particle, the two particles immediately (in the same time step) exchange their position. Note that when removing the colours, these rules are equivalent to the original rules (R1).

Let us now assume an injected particle to have reached at time $t - 1$ the end of the on-ramp L_2 such that L_1 is also occupied (and therefore $L_1 + 1$ is vacant). Hopping onto lane 1 from lane 2 at the end of the on-ramp creates at time t a blocked red particle at L_1 and a black particle at $L_1 + 1$. The colour exchange is equivalent to saying that the *black* particle moves onto $(L + 1)_1$, while the red particles moves onto L_1 .

In the next time step $t + 1$ the red particle on L_1 generates a red–black particle pair on $(L - 1)_1, L_1$ because of the oncoming black particle on lane 1 which interchanges position with the blocked red particle which was on L_1 at time t . It is now easy to see that the outgoing lane remains at density $\rho_{\text{out}} = 1/2$ with alternating black particles and vacancies. The current $j_{\text{out}} = 1/2$ is maximal. Any red particle that reaches L_2 jumps onto L_1 and then travels *backwards* along lane 1 with deterministic shock speed $v_s = -1$, since in each time step it is reached from behind by a black particle.

Therefore all particles entering lane 2 at the entrance point 0_2 end up in lane 1, filling it with a traffic jam moving backward. The density of red particles inside the jam is α ; they are geometrically distributed. Hence, the vacancies inside the jam are also geometrically distributed. The leftmost red particle which marks the end of the traffic jam may be defined as the microscopic position of the shock [25]. Its speed is -1 , in agreement with the general hydrodynamic result (2). The emerging congested domain eventually covers the entire lane to the left of L_1 . The stationary density in this domain is $\rho_1 = 1/2 + \alpha$ and the current is according to (1) $j_1 = 1/2 - \alpha$. The system is in the congested phase as predicted above. The time t^* at which stationarity is reached is $t^* \approx 2L$. The approximate sing becomes the random time $t \approx L$ at which the traffic jam on lane 1 is created.

- (b) Next we consider $\alpha = 1/2$. There is no need to introduce colours. It is easy to see that a fully occupied lane 1 up to site L_1 and the alternating particle–vacancy configuration on lane 2 and on the outgoing lane 1 are stationary. The system is in the congested phase.

From this description, however, it becomes by no means clear how the stationary state is reached in case (b). There is no reason to assume that for arbitrary ρ this happens after in one step as in case (a), with a fully blocked domain evolving backwards when the first traffic jam is formed. Instead, a more intricate sequence of relaxation cycles sets in as follows. We return to the hydrodynamic description in terms of macroscopic space and time coordinates and coarse-grained densities.

- (1) *Initialization.* The first step in the approach to stationarity consists of two stages: (i) the loading stage $0 < t < L$ and (ii) the development of a traffic jam during $L < t < cL$ with a constant c to be determined below. Initially, up to time $t = L$, nothing is different from the free-flow case. The system is in the loading stage described by (18) and (19). As soon as a stable back-moving traffic jam develops, the outflow onto lane 1 after the on-ramp becomes maximal, see the brief review of CA184 in section 2.1, with the difference that here the *front* of the congested region does not move backwards, but is stabilized at $x = L$ by the inflow of desperate particles coming from lane 2. Local stationarity in the vicinity of the end of the on-ramp requires the flux j_{jam} inside the evolving jam together with the flux $j_2 = 2\alpha\rho$ on lane 2 to match the outgoing flux $j_{\text{out}} = 1/2$. This yields

$$j_{\text{jam}} = 1/2 - 2\alpha\rho, \quad (22)$$

which implies for the density in the congested region

$$\rho_{\text{jam}} = 1/2 + 2\alpha\rho. \quad (23)$$

Hence, the shock moves backwards with speed given by (2)

$$v_{\text{init}} = \frac{1/2 - \alpha - \rho}{1/2 - \alpha - \rho + 4\alpha\rho}. \quad (24)$$

This shock reaches the beginning of the on-ramp $x = 0$ at time $t = L + L/|v_{\text{init}}|$ which yields $c = 1 - 1/v_{\text{init}} \geq 2$. During the development of the traffic jam along lane 1 of the two-lane segment, we therefore have

$$\rho_1(x, t) = \begin{cases} \rho & x < 0 \\ \alpha + \rho - 2\alpha\rho & 0 < x < L + v_{\text{init}}(t - L) \\ 1/2 + 2\alpha\rho & L + v_{\text{init}}(t - L) < x < L \\ 1/2 & t < x \end{cases} \quad (25)$$

and

$$\rho_2(x, t) = 2\alpha\rho. \quad (26)$$

Therefore at the end $t = cL$ of the initialization step, the densities of the two lanes are $\rho_1(x, cL) = 1/2 + 2\alpha\rho$ and $\rho_2(x, cL) = 2\alpha\rho$ which is in contrast to the free-flow phase where lane 1 is not congested. The initialization stages are illustrated in figure 4.

- (2) *Relaxation cycles* $t_k < t < t_k + 2L$. When the jam reaches the beginning of the on-ramp, the fraction of particles that move from lane 2 onto lane 1 after injection ceases to be $1 - 2\rho$ since the free-flow assumption with density ρ for lane 1 under which this was derived is no longer valid. From this instant of time, a relaxation cycle sets in; see figure 5 for illustration.

Each cycle has two stages, similar to the two previous initialization stages: (i) readjustment of the free-flow density of lane 2 and (ii) readjustment of the congested regime in lane 1. The incoming and outgoing lane segments do not change their state during the relaxation cycles and are not discussed in detail below.

Stage (i) of cycle k , $t_k < t < t_k + L$. At the end of cycle $k - 1$, the system is in a state similar to the end of the initialization stage (ii). The density on lane 2 adjusts itself to some value $\rho_2(k)$. This value is determined by appealing to local stationarity, i.e. balancing the current in the congested lane 1 such that the shock remains fixed (on a macroscopic scale) at $x = 0$. Hence, a density wave develops on lane 2 and moves forward with speed $+1$ until it reaches the end of the on-ramp $x = L$ at time $t_k + L$. The total current coming into the two-lane segment is the sum of the injection current α and j_{in} , i.e. $j_{\text{tot}} = \alpha + \rho$. Hence, stabilizing the shock position at $x = 0$ is achieved by adjusting

$$j_1(k - 1) + j_2(k) = \alpha + \rho, \quad (27)$$

such that the condition of vanishing shock velocity is satisfied. The density on lane 1 does not change during stage (i).

Stage (ii) of cycle k , $t_k + L < t < t_k + 2L$. When the density wave on lane 2 has reached $x = L$, the desperate cars lead to further blocking and a new traffic jam in the already congested lane 1 forms. This traffic jam moves backwards with speed -1 until it reaches $x = 0$ at time $t_k + 2L$. Then a new relaxation cycle sets in. Local stationarity at the end of the on-ramp $x = L$ requires that during stage (ii),

$$j_1(k) + j_2(k) = 1/2. \quad (28)$$

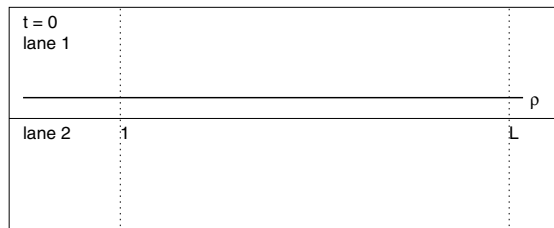
For the respective densities (remembering that lane 1 is congested and lane 2 is free), this yields

$$1 - \rho_1(k - 1) + \rho_2(k) = \alpha + \rho \quad (29)$$

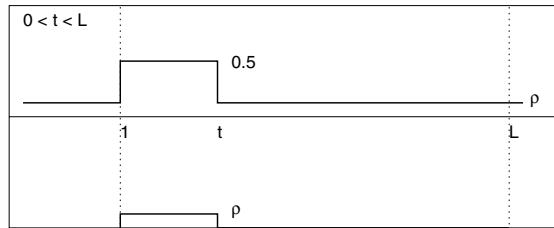
$$1 - \rho_1(k) + \rho_2(k) = 1/2. \quad (30)$$

Defining the initialization to represent the cycle number $k = 0$ with $\rho_1(0) = \rho_1(cL) = 1/2 + 2\alpha\rho$ and $\rho_2(0) = \rho_2(cL) = 2\alpha\rho$, this recursion is readily solved by

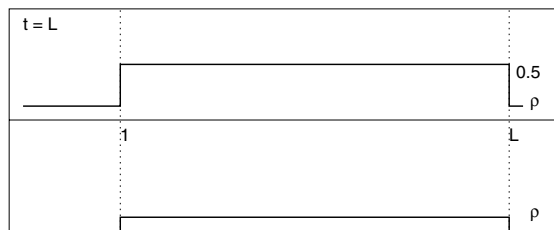
Density profiles for $\alpha = 1/2, 1/6 < \rho < 1/4$



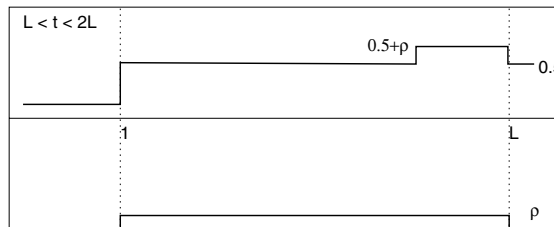
initial condition



density waves in both lanes with velocity $v=1$



initial loading of lane 2 after L steps



backmoving shock on lane 1 with speed $v=-1$; saturation of exit lane

Figure 4. Initial stages of the evolution of the density profile for $\alpha = 1/2$ in which case $c = 2$. The two stages are defined inside each figure.

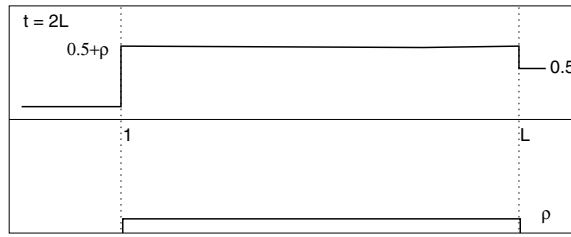
$$\rho_1(k) = (\alpha + \rho - 1/2)k + 2\alpha\rho + 1/2 \tag{31}$$

$$\rho_2(k) = (\alpha + \rho - 1/2)k + 2\alpha\rho. \tag{32}$$

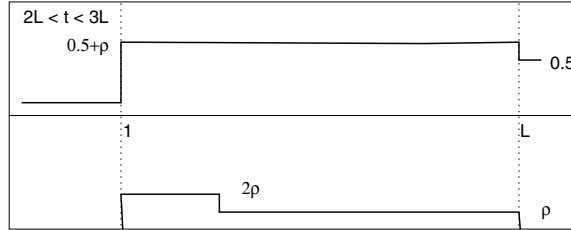
Since the first cycle starts at $t_1 = cL$, cycle k starts at time $t_k = L(c + 2(k - 1))$.

For the density profiles along the two-lane segment during the relaxation cycle k this gives during stage (i)

$$\rho_1(x, t) = \rho_1(k - 1) \quad 0 < x < L \tag{33}$$



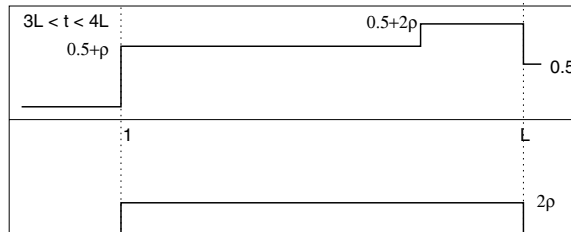
backmoving shock on lane 1 reaches entrance site 1



density wave on lane 2 with speed $v=1$ for $2p < 1/2$



density wave on lane 2 reaches merging point L



backmoving shock on lane 2 with speed $v=-1$

Figure 5. Relaxation cycle of the density profile for $\alpha = 1/2$, following the initialization stages shown in figure 4. The two stages of the cycle are defined inside each figure.

and

$$\rho_2(x, t) = \begin{cases} \rho_2(k) & 0 < x < \tilde{t}_k \\ \rho_2(k - 1) & \tilde{t}_k < x < L, \end{cases} \quad (34)$$

where $\tilde{t}_k = t - t_k$ is the elapsed time during cycle k . For stage (ii), we have

$$\rho_1(x, t) = \begin{cases} \rho_1(k - 1) & 0 < x < 2L - \tilde{t}_k \\ \rho_1(k) & 2L - \tilde{t}_k < x < L \end{cases} \quad (35)$$

and

$$\rho_2(x, t) = \rho_2(k) \quad 0 < x < L. \quad (36)$$

During stage (ii), $L < \tilde{t}_k < 2L$. The evolution (33)–(36) during a cycle is illustrated in figure 5 for $\alpha = 1/2$. After the completion of both cycles, the density in both lanes has increased. Correspondingly, the current in lane 2 has increased while in lane 1 it has decreased.

- (3) *Approach to stationarity* $t_{k^*+1} < t < t_{k^*+1} + 2L$. These cycles go on until the current inside the congested region is so low that condition (27) cannot be satisfied any longer with a new current (and hence density) on lane 2 that does not exceed the injection current α . The stopping condition $\rho_2(k^* + 1) > \alpha$ defines k^* as the last cycle that is completed. Inside the region of the phase diagram defined by

$$\frac{1}{k^*} < \frac{\alpha + \rho - 1/2}{\alpha(1 - 2\rho)} < \frac{1}{k^* + 1}, \quad (37)$$

the number of relaxation cycles is k^* . Note that $k^* = 0$ for

$$\rho > 1/[2(1 + 2\alpha)]. \quad (38)$$

Between this line in the phase diagram and the phase transition line $\alpha + \rho = 1/2$, there is an infinite family of dynamical phase transition lines at which the number of relaxation cycles increases by 1. As the phase transition line is approached, this number diverges. After cycle k^* a final relaxation process sets in, again consisting of two stages, see figure 6. In the case of $k^* = 0$, the approach to stationarity (3) immediately follows the initialization (1).

At the beginning of stage (i) of this final step a density wave with density α develops on lane 2 and propagates forward with speed +1, i.e. no particles move onto lane 1 any more at the beginning of the on-ramp. Therefore, at the same time $t_{k^*+1}^*$, the shock at $x = 0$ is no longer stationary, but starts moving into the ingoing lane with speed

$$v_{\text{trans}} = \frac{1 - \rho_1(k^*) - \rho}{\rho_1(k^*) - \rho} < 1. \quad (39)$$

When the density wave on lane 2 has reached $x = L$, this lane has become stationary. Then, at $t = t_{k^*+L}$ the second stage begins. A final shock is generated on lane 1 that moves backward with speed -1 and brings lane 1 into its stationary state with density ρ_1 . Full stationarity of the two-lane segment is thus reached at $t^* = t_{k^*+2L}$.

For the density profiles along the two-lane segment, this gives during stage (i)

$$\rho_1(x, t) = \rho_1(k^*) \quad 0 < x < L \quad (40)$$

and

$$\rho_2(x, t) = \begin{cases} \rho_2 & 0 < x < \tilde{t}_{k^*+1} \\ \rho_2(k^*) & \tilde{t}_{k^*+1} < x < L, \end{cases} \quad (41)$$

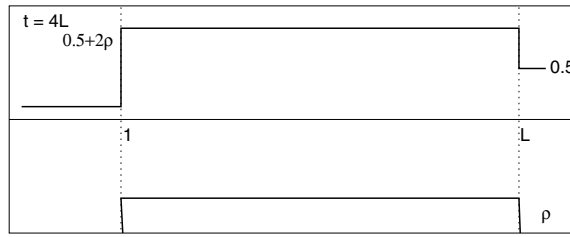
where $\tilde{t} = t - t_{k^*+1}$ is the elapsed time during the final relaxation step. For stage (ii), we have

$$\rho_1(x, t) = \begin{cases} \rho_1(k^*) & 0 < x < 2L - \tilde{t}_{k^*+1} \\ \rho_1 & 2L - \tilde{t}_{k^*+1} < x < L \end{cases} \quad (42)$$

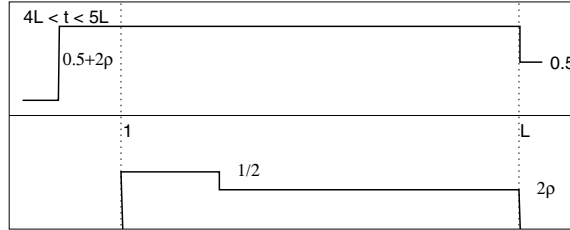
and

$$\rho_2(x, t) = \rho_2 \quad 0 < x < L. \quad (43)$$

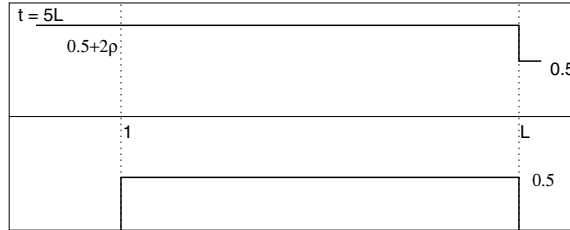
The approach to stationarity (40)–(43) is illustrated in figure 6 in the parameter range where $k^* = 1$.



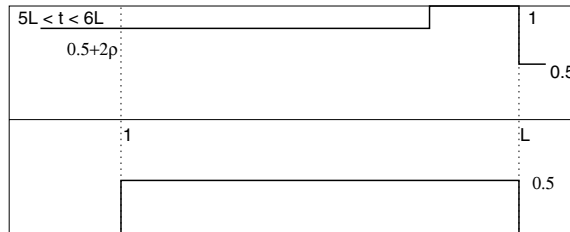
backmoving shock on lane 1 reaches entrance site 1



$3\rho > 1/2$: density wave on lane 2 with speed $v=1$
shock into entrance part of lane 1 with speed $v<0$



stationarity is reached on lane 2



backmoving shock on lane 1 with speed $v=-1$

Figure 6. Approach to stationarity of the density profile for $\alpha = 1/2$, following the relaxation cycle shown in figure 5. The two stages of the approach are defined inside each figure.

After the relaxation time t^* , the shock moves further into the ingoing lane 1 with speed -1 (figure 7). Eventually, it reaches the shock generated in stage 1 of the final step and continues to move indefinitely along the incoming lane as a single shock with speed

$$v_{\text{stat}} = \frac{1 - \rho_1 - \rho}{\rho_1 - \rho}. \tag{44}$$

This coalescence of shocks in CA184 is analogous to the coalescence of shocks on the hydrodynamic scale proved for the TASEP in [34]. After the initial loading stage, the

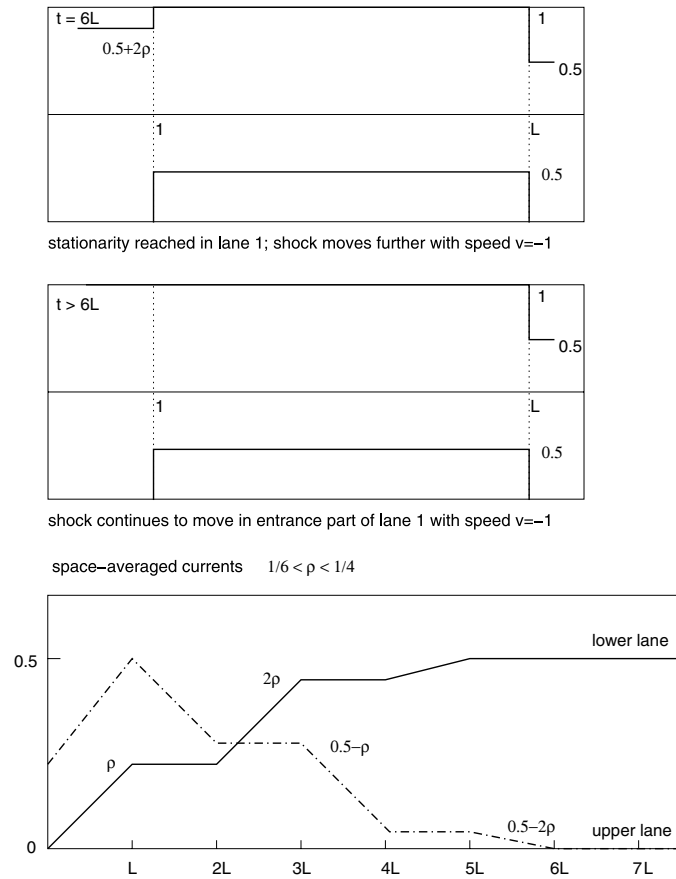


Figure 7. Penetration of the traffic breakdown into the incoming lane, following the approach to stationarity on the two-lane segment shown in figure 6 (top figures). (Bottom) Evolution of the current in the two lanes during the complete evolution.

space-averaged current on lane 1 decreases monotonically in a non-analytic fashion. Maximal injection $\alpha = 1/2$ leads to a complete breakdown on the traffic on lane 1 up to the end of the on-ramp (figure 7).

4.4. Simulation results

The results of the previous subsection are expected to be valid for an infinitely extended highway in the limit of a large number of lattice sites for the on-ramp. Bearing in mind that for traffic flow problems the natural lattice unit is the average length of a car the question arises what significance these results may have for on-ramps of a finite lattice size $L + 1$. (Here we return to microscopic lattice units.) We address this question by presenting snapshots of Monte Carlo simulations for $L = 100$ at various times for various parameter values.

In order to make the infinitely extended mathematical toy model accessible to Monte Carlo simulation, we have made the following modifications to the model.

- (a) We eliminate from the consideration all the particles that are present at time 0 at the sites of lane 1 to the right of 0_1 .

- (b) When a particle jumps to $(L+2)_1$, we eliminate it immediately from the model and declare the site $(L+2)_1$ empty.
- (c) We choose some value M and eliminate from the consideration all the particles that are present at time 0 at the sites of lane 1 to the left of $-M_1$.
- (d) At each time $t = 1, 2, \dots$, we check whether $-M_1$ was empty at time $t - 1$, and if yes, we insert a particle in $-M_1$ at time t with probability p_1 .

The first two modifications do not change the dynamics along the two-lane segment in any way as discussed above. The last two modifications are an exact representation of the dynamics of the original infinite model as long as no blocked particle is on $-M_1$, which means that no shock has reached this point of injection. This is not a serious limitation in practical terms as a shock enters the ingoing lane with non-negligible probability only in the final relaxation step of the congested phase, when the simulation is anyway stopped. The probability that it happens earlier by a large fluctuation in the incoming current decays exponentially in M . However, by analogy to CA184 with open boundaries, we do not expect even the presence of the shock at the injection point to cause a qualitative change of the behaviour of the model as long as $|M_1|$ is larger than the mean distance of the shock from the boundary (which is of order 1 and not growing with L).

With a view on simulations it is convenient to study the space-averaged densities $\rho_i(t) := 1/L \int_0^L dx \rho_i(x, t)$. In the absence of relaxation cycles (38), the relaxation takes place in four steps for which in the hydrodynamic limit one gets

$$\rho_1(t) = \begin{cases} \rho + \alpha(1 - 2\rho)t/L & 0 < t < L \\ \alpha + \rho - 2\alpha\rho + (\alpha + \rho - 1/2)(t/L - 1) & L < t < cL \\ 1/2 + 2\alpha\rho & cL < t < (c+1)L \\ \alpha(1 - 2\rho)(t/L - 1 - c) + 1/2 + 2\alpha\rho & (c+1)L < t < (c+2)L \end{cases} \quad (45)$$

$$\rho_2(t) = \begin{cases} 2\alpha\rho t/L & 0 < t < L \\ 2\alpha\rho & L < t < cL \\ \alpha(1 - 2\rho)(t/L - c) + 2\alpha\rho & cL < t < (c+1)L \\ \alpha & (c+1)L < t < (c+2)L. \end{cases} \quad (46)$$

Note that if all particles initially on \mathbb{Z}_1^+ are deleted, then the constant ρ in the first stage of $\rho_1(t)$ has to be replaced by $\rho t/L$.

To study the relaxation mechanism, we measured the total number of particles

$$N_2(t) = \sum_{i_2=1}^L n_{i_2}(t) \quad (47)$$

in lane 2 for $L = 100$. Each particle that has not immediately jumped to lane 1 after injection remains on lane 2 until it reaches the end of the on-ramp. Therefore, all remaining particles on the bulk part $1 \leq i_2 \leq L$ of the on-ramp become desperate once a jam on lane 1 is established (i.e. from stage 2 of the relaxation process onwards). Hence, the empirical density $\tilde{\rho}_2(t) = N_2(t)/L$ measures the increase in the number of desperate drivers which force their way onto lane 1, causing more disruption of the flow there in each cycle. Data are given in figure 8 for several randomly generated histories in the parameter range where $k^* = 1$. $N_2(t)$ has been averaged over a time window of ten time steps to reduce noise.

At the small lattice size $L = 100$, we do *not* expect the simulated data to be close to the hydrodynamic limit as given in (45) and (46). We find it remarkable that even though fluctuations are indeed strong, the cyclic structure of the relaxation is clearly visible in individual histories of the process, i.e. without ensemble averaging.

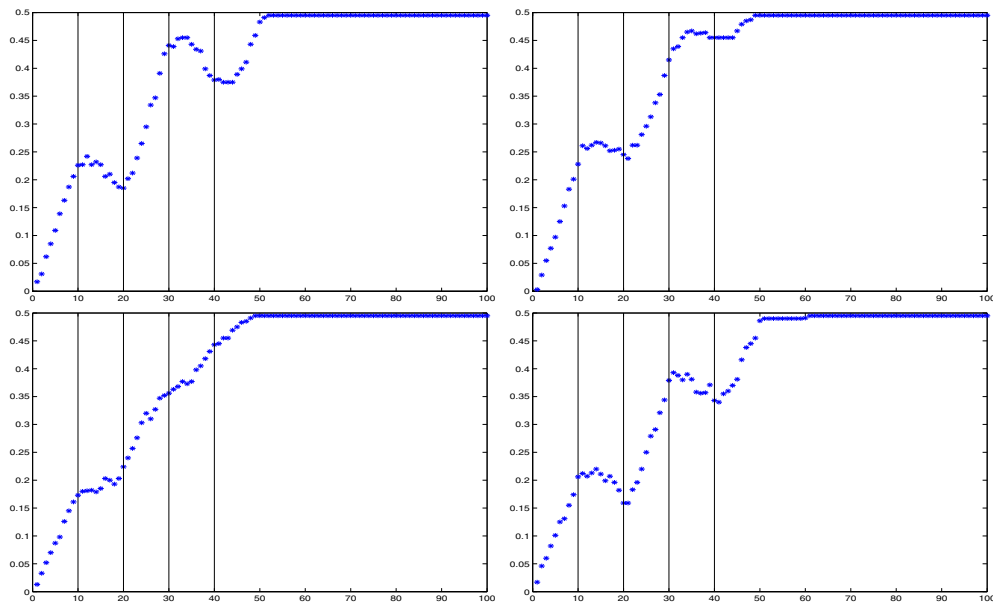


Figure 8. Monte Carlo simulation of the evolution of the empirical density $\bar{\rho}_2(t)$ on the on-ramp averaged over ten time steps versus time in units of ten steps, for $L = 100$, $\alpha = 1/2$, $\rho = 0.2$. Here $k^* = 1$ and $c = 2$. The vertical lines mark the end of each relaxation stage. The lane saturates at maximal density $1/2$ around $t = 500$. Four randomly generated histories are shown.

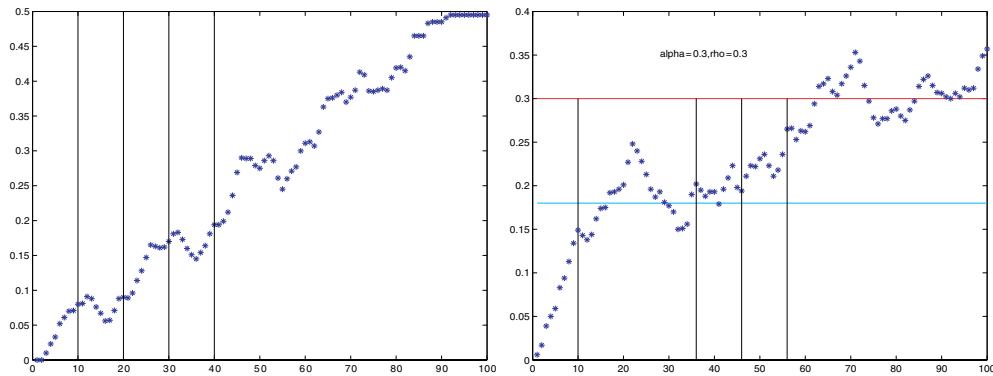


Figure 9. Monte Carlo simulation of the evolution of the empirical density $\rho_2(t)$ on the on-ramp for $L = 100$, averaged over ten time steps versus time in units of ten steps. The vertical lines mark the end of the first four relaxation stages. (Left) $\alpha = 1/2$, $\rho = 0.1$. The lane saturates at maximal density $1/2$ around $t = 900$ corresponding to $k^* = 3$. (Right) $\alpha = \rho = 0.3$, corresponding to $k^* = 1$ and $c = 3.6$. In (b) the horizontal line at $\bar{\rho}_2 = 0.18$ marks the constant hydrodynamic density during the second stage of the loading phase; the line at $\bar{\rho}_2 = 0.3$ marks the stationary density.

Closer to the phase transition line, the number of relaxation cycles increases in the hydrodynamic description. This is also reflected in finite chains as shown in figure 9(a) for $\alpha = 1/2$, $\rho = 0.1$. This is the transition point from $k^* = 3$ to $k^* = 4$. In the history of the process shown here, lane 2 relaxes at the time $t = 900$ corresponding to $k^* = 3$. In some simulations (not shown here), stationarity was not yet reached at this time. Also for noisy injection with $\alpha < 1/2$ some cyclicity remains recognizable despite strong noise, see figure 9(b).

This structure disappears as one goes to smaller values of α and smaller distance from the phase transition line.

5. Conclusions

The expected phase transition from free flow to the congested regime takes place when the incoming *initial* currents of the main road and the on-ramp equal the maximal output current of the main road. It is clear that a congested regime must exist when these two currents exceed the maximal output current. That the transition occurs exactly when they balance each other is a result of the microscopic lane-changing rules of the model.

The phase transition has novel interesting features. Inside the free-flow phase, the stationary distribution depends on the initial density ρ of particles on lane 1. In the congested phase, however, the memory of the initial distribution is lost. The stationary densities depend only on the injection strength α . A series of dynamical transitions takes place inside the congested phase. At these dynamical transition lines, the relaxation times change discontinuously as a result of an increasing integer number of relaxation cycles. This number diverges as the phase transition line to the free-flow phase is approached. These relaxation cycles are reminiscent of the ‘triggered stop-and-go waves’ discussed in the far more complex model of [2], but differ in that they do not persist, but drive the system into the homogeneous congested traffic state.

Interestingly, recent work on a two-component deterministic lattice gas with stochastic particle input at the system boundaries has also revealed relaxation cycles [31, 32]. In that model with two species of particles, there is a phase transition associated with spontaneous symmetry breaking. As the phase transition line is approached, the number of relaxation cycles diverges. At this point this is just an observation with no obvious link, as the phase transitions in these two models are rather different in nature. However, this coincidence suggests to study the phenomenon of relaxation cycles in deterministic cellular automata with stochastic boundaries under a more general perspective, e.g., by changing the microscopic lane-changing rules of the present model and by considering more elaborate exclusion processes that include next-nearest neighbour interaction [29, 35], varying intrinsic speeds [36] or slow-to-start rules [37].

It is clear that real automobile traffic is more noisy, and hence no idealized cyclic behaviour can be expected during the filling of a main road by inflow onto an on-ramp. In particular, the deterministic rule L2-b, which prevents the occurrence of a traffic jam on lane 2, suggests future work on a modified version of our model with a probabilistic analogue of rule L2-b and also the inclusion of ‘rude’ drivers who already force their way onto lane 1 before they reach the end of the on-ramp. The robustness of the cycles in the numerical simulation of our model is nevertheless intriguing. It would be interesting to investigate real traffic under conditions of sudden inflow onto an empty on-ramp in order to see whether flow patterns emerge that can be interpreted as a noisy version of idealized relaxation cycles. The number of ‘desperate’ drivers who manage to enter the main highway only at the end of an on-ramp could be a signature of such behaviour.

Acknowledgments

Financial support by CNPq, CAPES and FAPESP (VB and NM) and by DAAD, FAPESP and the Minerva-Einstein Center of the Weizmann Institute of Science (GMS) during various stages of this work is gratefully acknowledged. GMS thanks the Institute of Mathematics

and Statistics of the University of São Paulo and the Weizmann Institute of Science for kind hospitality. We thank D Helbing and A Schadschneider for useful comments.

References

- [1] Popkov V, Santen L, Schadschneider A and Schütz G M 2001 Empirical evidence for a boundary-induced nonequilibrium phase transition *J. Phys. A: Math. Gen.* **34** L45–52
- [2] Helbing D, Hennecke A and Treiber M 1999 Phase diagram of traffic states in the presence of inhomogeneities *Phys. Rev. Lett.* **82** 4360–3
- [3] Schütz G and Domany E 1993 Phase-transitions in an exactly soluble one-dimensional exclusion process *J. Stat. Phys.* **72** 277–96
- [4] Derrida B, Evans MR, Hakim V and Pasquier V 1993 Exact solution of a 1d asymmetric exclusion model using a matrix formulation *J. Phys. A: Math. Gen.* **26** 1493–517
- [5] Kolomeisky A B, Schütz G M, Kolomeisky E B and Straley J P 1998 Phase diagram of one-dimensional driven lattice gases with open boundaries *J. Phys. A: Math. Gen.* **31** 6911–9
- [6] Bahadoran C 2006 Hydrodynamics and hydrostatics for a class of asymmetric particle systems with open boundaries *Preprint math.PR/0612094*
- [7] Lighthill M J and Witham G B 1955 On kinematic waves: II. A theory of traffic flow on long crowded roads *Proc. R. Soc. Lond. A* **229** 317–45
- [8] Chowdhury D, Santen L and Schadschneider A 2000 Statistical physics of vehicular traffic and some related systems *Phys. Rep.* **329** 199–329
- [9] Helbing D 2001 Traffic and related self-driven many-particle systems *Rev. Mod. Phys.* **73** 1067–141
- [10] Pronina E and Kolomeisky A B 2005 Theoretical investigation of totally asymmetric exclusion processes on lattices with junctions *J. Stat. Mech: Theor. Exp.* P07010
- [11] Huang D W 2006 Ramp-induced transitions in traffic dynamics *Phys. Rev. E* **73** 016123
- [12] Jiang R, Wu Q S and Wang B H 2002 Cellular automata model simulating traffic interactions between on-ramp and main road *Phys. Rev. E* **66** 036104
- [13] Huang D W 2005 Analytical results of asymmetric exclusion processes with ramps *Phys. Rev. E* **72** 016102
- [14] Ciamarra M P 2005 Optimizing on-ramp entries to exploit the capacity of a road *Phys. Rev. E* **72** 066102
- [15] Diedrich G, Santen L, Schadschneider A and Zittartz J 2000 Effects of on- and off-ramps in cellular automata models for traffic flow *Int. J. Mod. Phys. C* **11** 335–45
- [16] Campari E G and Levi G 2000 A cellular automata model for highway traffic *Eur. Phys. J. B* **17** 159–66
- [17] Pedersen M M and Ruhoff P T 2002 Entry ramps in the Nagel–Schreckenberg model *Phys. Rev. E* **65** Art. No. 056705
- [18] Nassab K, Schreckenberg M, Ouaskit S and Boulmakoul A 2005 Impacts of different types of ramps on the traffic flow *Physica A* **352** 601–11
- [19] Jia B, Jiang R and Wu Q S 2005 The effects of accelerating lane in the on-ramp system *Physica A* **345** 218–26
- [20] Jiang R and Wu Q S 2006 Phase transition at an on-ramp in the Nagel–Schreckenberg traffic flow model *Physica A* **366** 523–9
- [21] Wolfram S 1983 Statistical mechanics of cellular automata *Rev. Mod. Phys.* **55** 601
- [22] Belitsky V, Krug J, Neves E J and Schütz G M 2001 A cellular automaton model for two-lane traffic *J. Stat. Phys.* **103** 945–71
- [23] Belitsky V and Ferrari P A 1995 Ballistic annihilation and deterministic surface growth *J. Stat. Phys.* **80** 517–43
- [24] Belitsky V and Ferrari P A 2005 Invariant measures and convergence for cellular automaton 184 and related processes *J. Stat. Phys.* **118** 589–623
- [25] Belitsky V, Marić N and Schütz G M Shock motion and rarefaction waves in CA184, in preparation
- [26] Schütz G 1993 Time-dependent correlation-functions in a one-dimensional asymmetric exclusion process *Phys. Rev. E* **47** 4265–77
- [27] Evans M R, Rajewsky N and Speer E R 1999 Exact solution of a cellular automaton for traffic *J. Stat. Phys.* **95** 45–96
- [28] de Gier J and Nienhuis B 1999 Exact stationary state for an asymmetric exclusion process with fully parallel dynamics *Phys. Rev. E* **59** 4899–911
- [29] de Gier J 2001 Exact stationary state for a deterministic high-speed traffic model with open boundaries *J. Phys. A: Math. Gen.* **34** 3707–20
- [30] Hager J S 2001 Extremal principle for the steady-state selection in driven lattice gases with open boundaries *Phys. Rev. E* **63** 067103
- [31] Willmann R D, Schütz G M and Grosskinsky S 2005 Dynamical origin of spontaneous symmetry breaking in a field-driven nonequilibrium system *Europhys. Lett.* **71** 542–8

- [32] Großkinsky S, Schütz G M and Willmann R D 2007 Rigorous results on spontaneous symmetry breaking in a one-dimensional driven particle system *J. Stat. Phys.* **128** 587–606
- [33] Rajewsky N, Santen L, Schadschneider A and Schreckenberg M 1998 The asymmetric exclusion process: comparison of update procedures *J. Stat. Phys.* **92** 151–94
- [34] Ferrari P A, Fontes L R G and Vares M E 2000 The asymmetric simple exclusion model with multiple shocks *Ann. Inst. Henri Poincaré—PR* **36** 109–26
- [35] Antal T and Schütz G M 2000 Asymmetric exclusion process with next-nearest-neighbor interaction: some comments on traffic flow and a nonequilibrium reentrance transition *Phys. Rev. E* **62** 83-93
- [36] Nagel K and Schreckenberg M 1992 A cellular automaton model for freeway traffic *J. Phys.* **1** 2 2221–9
- [37] Nishinari K, Fukui M and Schadschneider A 2004 A stochastic cellular automaton model for traffic flow with multiple metastable states *J. Phys. A: Math. Gen.* **37** 3101–10